Premature ovarian aging in mice deficient for *Gpr3*

Catherine Ledent*†, Isabelle Demeestere‡, David Blum*§, Julien Petermans*, Tuula Hämäläinen¶, Guillaume Smits*‖, and Gilbert Vassart*‖

*Institut de Recherches en Biologie Humaine et Moléculaire, ‡Research Laboratory on Human Reproduction, §Laboratory of Experimental Neurosurgery, and ‖Department of Medical Genetics, Hôpital Erasme, University of Brussels, Campus Erasme, 808 Route de Lennik, B-1070 Brussels, Belgium; and ¶Institute of Biomedicine, University of Turku, Kiinamyllynkatu 10, 20520, Turku, Finland

Communicated by Etienne-Emile Baulieu, Collège de France, Le Kremlin-Bicêtre, France, May 9, 2005 (received for review February 14, 2005)

After becoming competent for resuming meiosis, fully developed mammalian oocytes are maintained arrested in prophase I until ovulation is triggered by the luteotropin surge. Meiotic pause has been shown to depend critically on maintenance of cAMP level in the oocyte and was recently attributed to the constitutive Gs (the heterotrimeric GTP-binding protein that activates adenylyl cyclase) signaling activity of the G protein-coupled receptor GPR3. Here we show that mice deficient for *Gpr3* are unexpectedly fertile but display progressive reduction in litter size despite stable age-independent alteration of meiotic pause. Detailed analysis of the phenotype confirms premature resumption of meiosis, *in vivo*, in about one-third of antral follicles from *Gpr3*$^{-/-}$ females, independently of their age. In contrast, in aging mice, absence of GPR3 leads to severe reduction of fertility, which manifests by production of an increasing number of nondeveloping early embryos upon spontaneous ovulation and massive amounts of fragmented oocytes after superovulation. Severe worsening of the phenotype in older animals points to an additional role of GPR3 related to protection (or rescue) of oocytes from aging. *Gpr3*-defective mice may constitute a relevant model of premature ovarian failure due to early oocyte aging.

infertility | meiosis | cAMP | G protein-coupled receptor | fragmented oocytes

Meiosis in mammalian oocytes starts during embryonic life and pauses around birth in the diplotene stage of prophase I (1). Thereafter, oocytes are recruited continuously to reacquire meiotic competence at a follicular development stage, corresponding roughly to the appearance of the antrum (2). Meiotic arrest is maintained in competent oocytes until the luteinizing hormone surge (3), which causes ovulation and leads to progression of meiosis to metaphase II. Release from this second meiotic arrest occurs only upon fertilization (1). There is compelling evidence that concentration of cAMP in the oocyte is a key parameter for maintenance of meiotic arrest in competent oocytes (1, 4), probably via phosphorylation of specific proteins by protein kinase A (5–7). Direct implication of the balance between cAMP generation by adenylyl cyclase 3 isoform and degradation by phosphodiesterase 3 have been demonstrated (8–10). The steady-state concentration of cAMP in the oocytes is regulated by the interplay of signals originating both in follicular cells and the oocytes themselves (1, 11). Although some evidence indicates that cAMP from follicular cells can traverse gap junctions (12), several studies support the view that production of cAMP by the oocyte itself is essential to maintaining meiotic arrest. Microinjection of oocytes with antibodies neutralizing the activity of Gs (the heterotrimeric GTP-binding protein that activates adenylyl cyclase) causes meiosis resumption in intact follicles (13). Stimulation by insulin-like 3 of LGR8, a G protein-coupled receptor present in the oocyte, was shown to cause meiotic progression by activation of the inhibitory G protein Gi (14). Finally, GPR3, a G protein-coupled receptor (15) endowed with constitutive Gs signaling activity (16, 17), was recently shown to be expressed in the oocyte and to play a key role in preventing premature resumption of meiosis in antral follicles (18).

To address the physiological importance of this receptor, we generated mice lacking *Gpr3* and explored the consequences of GPR3 deficiency on reproduction. We found that, besides its contribution to meiotic arrest in antral follicles, GPR3 plays a key role in the establishment of embryonic developmental competence and maintenance of fertility in aging female mice.

Materials and Methods

Generation of *Gpr3*$^{-/-}$ Mice. Mouse *Gpr3* was disrupted by using a gene-replacement vector that deleted the entire coding sequence (see *Supporting Text*, which is published as supporting information on the PNAS web site).

Production of Staged Embryos. For RNA extraction, all oocytes and embryos were collected from 6-week-old wild-type spontaneously cycling CD1 mice. Oocytes were obtained by hyaluronidase treatment (0.3 mg/ml) of cumulus masses the day of the vaginal plug [0.5 days postcoitus (dpc)]. Absence of follicular cells was carefully checked under a microscope. Two-cell stage embryos and morulae were collected by flushing oviducts on 1.5 and 2.5 dpc, respectively. Blastocysts were flushed from the uterus on 4 dpc. Oocytes/embryos were frozen and conserved in liquid N_2 until RNA extraction.

RT-PCR. Poly(A)+ RNA was extracted from 60–150 mouse embryos by using the Fast Tract RNA purification kit (Invitrogen) and reverse-transcribed with Superscript II (Invitrogen) by using oligo(dT) 12–18 primers. An equivalent of three to eight embryos was used for PCR. *Gpr3* and *β-actin* primers as well as PCR reaction parameters were as shown in Table 1, which is published as supporting information on the PNAS web site. PCR reaction products were analyzed by electrophoresis on 1.2% agarose gel stained with ethidium bromide to visualize products on a UV transilluminator. A single product of 612 and 243 bp was amplified for *Gpr3* and *β-actin* cDNAs, respectively.

Morphology. For conventional light microscopy, 6-μm sections of 4% formaldehyde-fixed paraffin-embedded tissues were stained with haematoxylin/eosin. For immunofluorescence detection of GPR3, oocytes were fixed by using 4% paraformaldehyde PBS solution and then stored or processed in a washing blocking solution (19). The standard-labeling procedure was performed by using anti-GPR3 polyclonal antibody (diluted 1:100, Lifespan Biosciences) and FITC-conjugated donkey anti-rabbit IgG (diluted 1:200, Jackson ImmunoResearch Laboratories). Processing of oocytes/embryos for immunofluorescence detection of α-tubulin was performed as described (19) by using a monoclonal anti-α-tubulin (1:100 dilution; Sigma) followed by Alexafluor 488 goat anti-mouse IgG (1:200 dilution, Molecular Probes). DNA was counterstained with 1 μM ethidium homodimer-2 (Molecular Probes) and oocytes/embryos were

Freely available online through the PNAS open access option.

Abbreviation: GV, germinal vesicle.

†To whom correspondence should be addressed. E-mail: cledent@ulb.ac.be.

mounted onto polyL-lysine coated slides by using Vectashield (Vector Laboratories). The specimens were examined under a Bio-Rad 124 UV confocal laser microscope, and the images were processed by using LASERSHARP software, Ver. 3.0 (Bio-Rad).

Collection of Antral Stage Oocytes. Twenty-four-day- and 6-month-old mice of both genotypes were primed 48 h previously with 5 units of pregnant mare's serum gonadotropin (Folligon, Intervet, Mechelen, Belgium). Ovaries were removed in 10% FCS M2 medium (Specialty Media, Phillipsburg, NJ) containing 300 μM dibutyryl cAMP (Sigma) to maintain meiotic arrest. Oocytes were collected by puncturing medium and large antral follicles (follicles with diameters $\geq$190 μm) and cultured for 18 h in groups of 5 in 20 μl of 10% FCS Minimal Essential Medium (MEM GlutaMAX, Life Technologies, Grand Island, NY) under paraffin oil, at 37.5°C, 5% CO_2 + 95% air with maximal humidity. Oocyte nuclear maturation stage was evaluated at the collection time and after 18 h of culture.

Superovulation. Mice were superovulated with 5 units of pregnant mare's serum gonadotropin (Folligon, Intervet) followed by 5 units of human chorionic gonadotropin (hCG, Chorulon, Intervet) 48 h later. Each female was placed in a cage with one vasectomized male and checked the next morning for a copulation plug. Cumulus–oocyte complexes were collected from the oviducts 16 h after hCG injection.

***In Vitro* Culture of Embryos.** Fertilized eggs were harvested from the ampullae of mice after successful mating as assessed by the presence of mating plugs. Cumulus cells were removed by pipetting after brief incubation in 0.3 mg/ml hyaluronidase (Sigma) in M2 medium (Specialty Media). Washed embryos were incubated in 30-μl droplets of preequilibrated KSOM (Specialty Media), covered with mineral oil at 37°C in a humidified atmosphere of 5.5% CO_2 in air.

Visualizing Early Embryo Implantation Sites. Implantations regions were identified at 5.5 days postcoitus after injection of 0.1-ml Chicago blue B dye (1% solution into saline) in the tail vein 5–10 min before killing (20).

Follicle-Stimulating Hormone Measurements. Blood samples were collected from 8.5-month-old cycling mice in diestrus. Serum was prepared and stored at −20°C until assayed, as described (21).

Estrous Cycle. Assessment of estrous cycle stages and length was made by histology analysis of vaginal smears taken daily for a period of 21 days.

Statistical Analysis. Percentages were compared with the use of χ^2 test and Cochran–Armitage trend test. Preimplantation embryonic development stages were analyzed with ANOVA tests for repeated measures (stages at three levels) with two between-groups factors (age at three levels and genotype at two levels). Postimplantation embryonic development data were analyzed with ANOVA tests with the following factors: genotype, stage, age, and their two-way interactions. The same kind of analysis was then performed for each genotype separately.

Results and Discussion

Accelerated Age-Dependent Reduction of Fertility in *Gpr3*$^{-/-}$ Females. *Gpr3*$^{-/-}$ animals were viable and exhibited no obvious growth, developmental, hematological, or biochemical abnormalities. Homozygote offspring were generated from heterozygotes with minimal deviation from the expected Mendelian frequency (22.1%, n = 503). Spontaneously cycling *Gpr3*$^{-/-}$ females exhibited progressive reduction in litter size with advancing maternal age (Fig. 1*A*). This reduction was independent

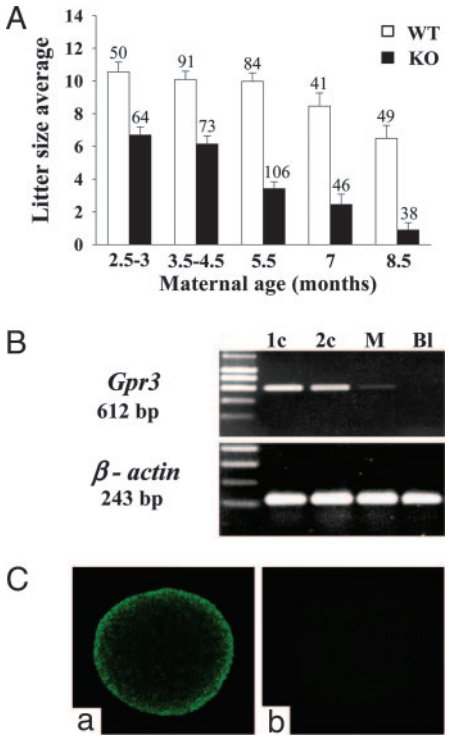

Fig. 1. Aging *Gpr3*$^{-/-}$ mice display accelerated reduction of fertility, and *Gpr3* is expressed in mouse oocytes and two-cell embryos. (*A*) Litter size resulting from *Gpr3*$^{+/+}$ (open columns) and *Gpr3*$^{-/-}$ (black columns) incrosses as a function of maternal age. Results show a clear difference between the two genotypes at all ages ($P < 0.001$), and the difference increases with age. Only animals showing spontaneous ovarian cycles were scored. Results are expressed as mean ± SEM. The number of mothers in each group is indicated at the top of the columns. (*B*) RT-PCR detection of *Gpr3* and *β-actin* mRNAs in preimplantation *Gpr3*$^{+/+}$ embryos at different stages (1c, one cell; 2c, two cell; M, morula; and Bl, blastocyst). (*C*) Detection of GPR3 on the wild-type oocyte by immunofluorescence confocal microscopy by using an anti-GPR3 polyclonal antibody (*a*). Incubation of the oocyte with the second antibody alone yielded only a background signal (*b*).

of the genotype of the sperm (Tables 2 and 3, which are published as supporting information on the PNAS web site). The receptor is present in oocytes and early embryos of wild-type mice. As shown in Fig. 1*B*, *Gpr3* transcripts were readily detected by RT-PCR in wild-type one- and two-cell embryos. Only trace amounts of the mRNA remained in morulae, and it was absent in blastocysts. The receptor protein was detected at the surface of unfertilized oocytes by immunocytochemistry (Fig. 1*C*).

Age-Independent Premature Resumption of Meiosis I and Impaired Meiotic Competence of *Gpr3*$^{-/-}$ Oocytes. With the aim of identifying the mechanism responsible for the age-dependent effect of GPR3 deficiency on fertility, we analyzed oocytes retrieved from medium and large antral follicles of 3.5-week- and 6-month-old animals and maintained in culture for 18 h. Such oocytes should display a germinal vesicle (GV) at collection time, whereas GV breakdown (GVB) and extrusion of the first polar body would indicate progression to metaphase II. For both maternal ages tested, an important decrease in the percentage of GV-stage oocytes was observed in *Gpr3*$^{-/-}$ mice, concomitant with an increase in the number of oocytes having undergone GVB, extruded one or two polar bodies, or presenting morphological abnormalities (i.e., fragmentation or lysis) (Fig. 2). These observations demonstrate that, at both ages, about one-third of antral stage *Gpr3*$^{-/-}$ oocytes experience precocious ripening *in vivo*, thus confirming that GPR3 is one of the agents responsible

DEVELOPMENTAL BIOLOGY

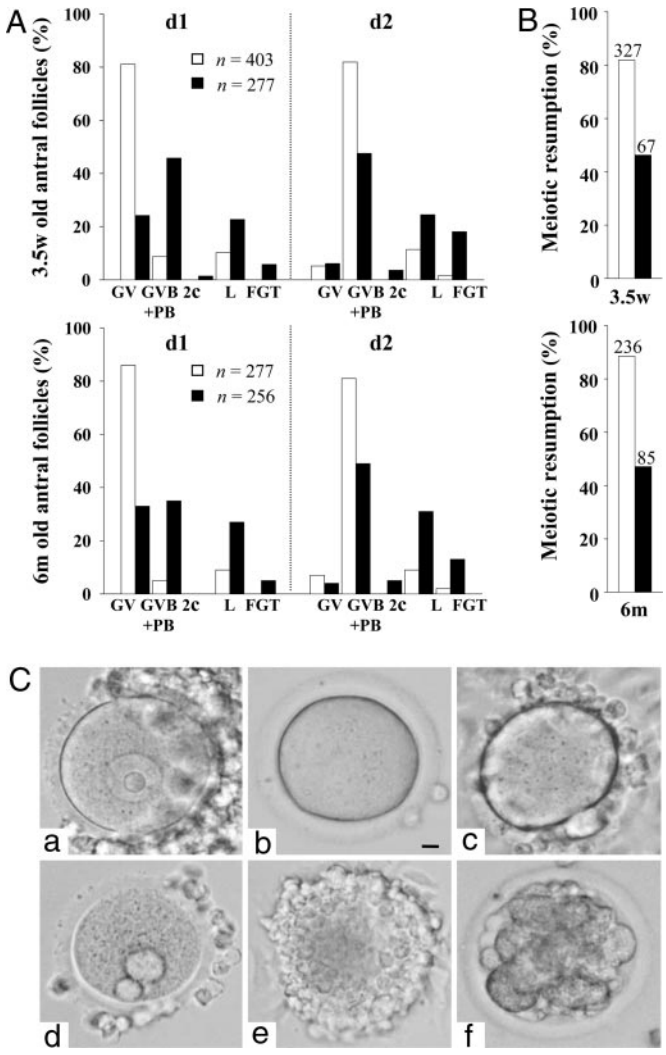

Fig. 2. Oocytes from *Gpr3*$^{-/-}$ mice display age-independent premature resumption of meiosis I, associated with increase in morphological abnormalities. (*A*) Antral oocytes from 3.5-week (3.5w)- and 6-month (6m)-old ovaries were collected and scored for presence of a GV, GV breakdown (GVB), or extrusion of first polar body (PB) at collection time (d1) and after 18 h in culture (d2). The proportion of oocytes undergoing parthenogenetic division (2c), lysis (L), or fragmentation (FGT) was also scored. For both ages, a clear decrease in the proportion of GV stage was observed in *Gpr3*$^{-/-}$ oocytes ($P < 0.001$) at collection time (d1); spontaneous resumption of meiosis was impaired after 18 h in culture (d2). (*B*) Meiotic competence expressed as percentage of GV stage oocytes having extruded the first polar body after 18 h in culture. For *A* and *B*, open columns, *Gpr3*$^{+/+}$ and black columns, *Gpr3*$^{-/-}$ animals. (*C*) Representative morphology of oocytes observed in light microscopy by using Nomarski optics. (*a*) Oocyte with GV intact, (*b*) oocyte showing GV breakdown, (*c*) oocyte with first polar body extruded, (*d*) oocyte with two polar bodies extruded, (*e*) lysed oocyte, and (*f*) fragmented oocyte. (Bar, 10 μm.)

for cAMP-dependent maintenance of meiotic arrest. The population of antral follicles that we studied (follicles with diameter $\geq$190 μm) could explain the lower percentage of meiotic resumption observed in our *Gpr3*$^{-/-}$ oocytes compared with Mehlmann *et al.* (18). That only a fraction of oocytes is affected indicates, however, that GPR3-independent mechanisms, extrinsic or intrinsic to the oocyte, may compensate partially for the loss of GPR3 expression, probably by maintaining cAMP concentration in nonprogressing oocytes above the threshold required for meiotic arrest. Besides, and quite unexpectedly, whereas one-third of them show early resumption of meiosis, when taken globally, *Gpr3*$^{-/-}$ oocytes at the GV stage display impaired meiotic competence. Indeed, during culture *ex vivo*, only 50% of *Gpr3*$^{-/-}$ oocytes resume meiosis spontaneously, compared with 80% of *Gpr3*$^{+/+}$ (Fig. 2*B*). The stable proportion of oocytes showing these phenomena, independently of age, does not account for the progressive decrease in fertility observed in aging *Gpr3*$^{-/-}$ females. Our observations agree with those of Mehlmann *et al.* (18), indicating that functional GPR3 is required to ensure meiotic pause. In addition, they demonstrate that it is also required to establish or maintain meiotic competence and to compensate for age-dependent decrease in oocyte quality.

Age-Dependent Increase of Fragmented Oocytes in Superovulated *Gpr3*$^{-/-}$ Females. The effect of GPR3 deficiency was then assessed on the number and morphology of eggs resulting from spontaneous or experimentally induced ovulation. In both conditions, the number of oocytes produced per ovulating *Gpr3*$^{-/-}$ or *Gpr3*$^{+/+}$ animal was similar, whatever their age (Table 4, which is published as supporting information on the PNAS web site). Oocytes collected in the ampullae of spontaneously ovulating *Gpr3*$^{-/-}$ mice displayed only a minor rate of fragmentation or abnormalities, which increased slightly with age (from 7% at 2.5 months to 13% at 8.5 months; Table 5, which is published as supporting information on the PNAS web site). In contrast, after stimulation, very high rates of fragmentation were observed, and this phenotype displayed severe worsening with age, reaching 46% at 10 months (Fig. 3*A*; Table 6, which is published as supporting information on the PNAS web site). By comparison, upon stimulation, *Gpr3*$^{+/+}$ mice produced only a minority of fragmented oocytes, and the phenomenon became apparent only in 5-month-old animals (Fig. 3*A*). These observations indicate that natural ovulation cycles recruit *Gpr3*$^{-/-}$ oocytes that are less affected by GPR3 deficiency. In contrast, superovulation mobilizing follicles that would otherwise have become atretic, recruit a larger proportion of abnormal oocytes, probably secondary to premature ripening or maturational incompetence. The progressive worsening of the phenotype of superovulated *Gpr3*$^{-/-}$ oocytes with age is compatible with the following hypotheses: sustained GPR3 activity could be needed during follicular development to prevent aging of oocytes. Alternatively, it could act during the antral phase to reverse deleterious effects of aging. According to current knowledge, in mice, superovulated oocytes are known to be of poorer quality than spontaneously ovulated eggs (22, 23), a characteristic that increases with maternal age (24–26). Our results suggest that GPR3 dysregulation might be one of the factors implicated in these phenomena, which agrees with the notion that older females would produce an increased proportion of atretic and less competent oocytes (25–27).

Age-Dependent Reduction of Developmental Capacity of *Gpr3*$^{-/-}$ Embryos. We next examined the preimplantation developmental capacity and implantation frequency of embryos in *Gpr3*$^{+/+}$ and *Gpr3*$^{-/-}$ females at different maternal ages. The ability of zygotes to progress along embryonic development was scored by counting, for each step, the number of progressing embryos (Fig. 4 and Table 4). Embryos from *Gpr3*$^{-/-}$ mothers completed transition from zygote stage to blastocyst with significantly lower frequency, compared with controls ($P < 0.001$). This developmental failure was characterized by the progressive appearance with age of degenerated and/or fragmented embryos all along preimplantation development (Fig. 4 *A*, *C*, and *D*; Table 4). It was mainly accounted for by a lower frequency of progression of the unicellular zygote to the two-cell stage (Fig. 4*B*). Interestingly, the embryos from *Gpr3*$^{-/-}$ mothers, which succeeded in reaching the blastocyst

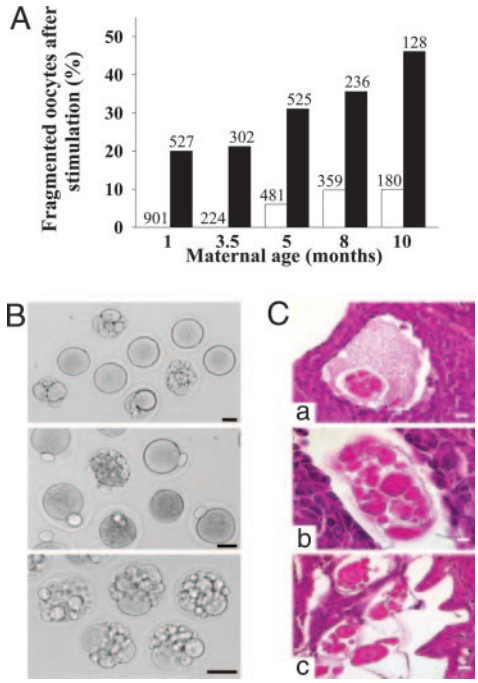

Fig. 3. Oocytes from superovulated *Gpr3*$^{-/-}$ females display age-dependent increase in fragmentation. (*A*) Percentage of fragmented unfertilized oocytes collected in the ampullae of females at different ages after exogenous hormonal stimulation. Total number of oocytes analyzed is indicated above the columns (open columns, *Gpr3*$^{+/+}$; black columns and *Gpr3*$^{-/-}$, oocytes). Whereas both genotypes produced progressively more fragmented oocytes with age ($P < 0.001$), at all ages, *Gpr3*$^{-/-}$ animals produced much more fragmented oocytes than *Gpr3*$^{+/+}$ ($P < 0.001$). (*B*) Nonfertilized *Gpr3*$^{-/-}$ oocytes observed in light microscopy by using Nomarski optics at time of harvest in the ampullae of superovulated females. Normally shaped unfertilized oocytes with or without polar body, fragmented oocytes, and oocytes exhibiting cytoplasmic condensation are observed. (Bar, 40 μm.) (*C*) Histology sections of *Gpr3*$^{-/-}$ fragmented oocytes observed in follicles (*a* and *b*) and oviducts (*c*) after stimulation by human chorionic gonadotropin. [Bars, (*a–c*) 20 μm and (*b*) 10 μm.]

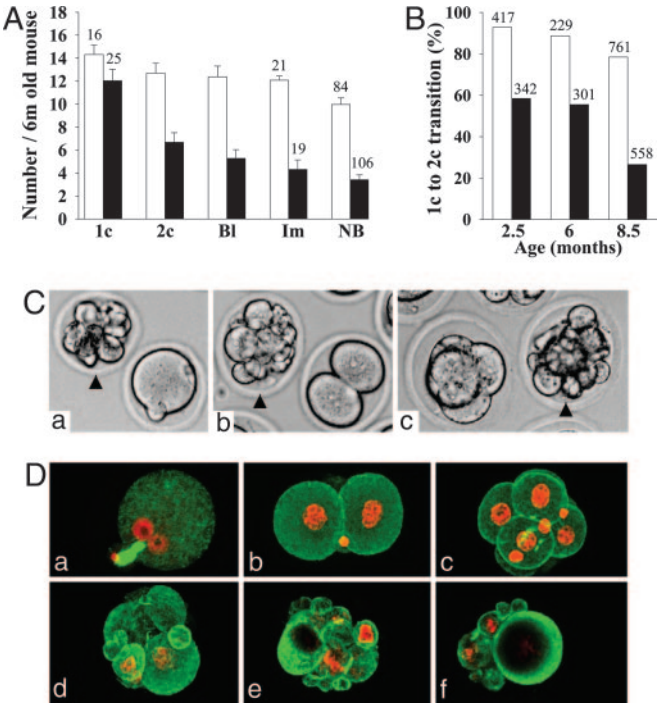

Fig. 4. Decreased fertility of aged *Gpr3*$^{-/-}$ females is accounted for by reduction of zygote—early-embryo transition. (*A*) Number of zygotes produced by spontaneous ovulation (1c), embryonic preimplantation developmental capacity to the two-cell (2c) and blastocyst stages (Bl), number of implanted embryo (Im) and litter size (NB) are indicated for 6-month-old *Gpr3*$^{+/+}$ (open columns) and *Gpr3*$^{-/-}$ females (black columns) mated with males of the same genotype. Results are expressed as the mean ± SEM, with the number of mothers tested indicated at the top of the columns. Transition from 1c to 2c stage was strongly decreased in *Gpr3*$^{-/-}$ embryos ($P < 0.001$), as compared with *Gpr3*$^{+/+}$ ($P = 0.400$), whereas the 2c-to-blastocyst transition was not significantly different for both genotypes (*Gpr3*$^{+/+}$, $P = 0.966$; *Gpr3*$^{-/-}$, $P = 0.492$). Similarly, the decrease observed between the number of implantation sites and litter size was not significantly different in the two genotypes (*Gpr3*$^{+/+}$, $P = 0.062$; *Gpr3*$^{-/-}$, $P = 0.404$). (*B*) The percentage of zygotes displaying progression to the two-cell stage in spontaneously ovulating females was much decreased in *Gpr3*$^{-/-}$ animals at all maternal ages tested ($P < 0.001$), and the decrease was more important at 8.5 months of age. The total number of embryos analyzed is indicated above the columns (open columns, *Gpr3*$^{+/+}$; black columns and *Gpr3*$^{-/-}$). (*C*) Photomicrographs showing coexistence of normally shaped *Gpr3*$^{-/-}$ one-cell (*a*), two-cell (*b*) and four-cell embryos (*c*) with *Gpr3*$^{-/-}$ fragmented embryos (arrowheads), after spontaneous ovulation, in 6-month-old females. (*D*) Laser-scanning confocal microscopy of *Gpr3*$^{-/-}$ preimplantation embryos after immunofluorescent staining for α-tubulin (green). DNA was counterstained with ethidium homodimer-2 (red). Normally shaped (*a–c*) and degenerated *Gpr3*$^{-/-}$ embryos (*d–f*) are illustrated: (*a*) zygote with male and female pronuclei, each displaying a large nucleolus; only the second polar body is visible; (*b*) two-cell embryo; and (*c*) six-cell embryo. (*d–f*) Fragmented embryos with most of the fragments containing chromatin material.

stage, implanted and developed into newborns with normal frequency. As seen for the reduction of fertility (Tables 2 and 3), the above results were independent of the genotype of the mating males (data not shown). They qualify *Gpr3* as a maternal effect gene displaying a major and increasing role in aging females and with its main impact on the zygote—two-cell transition. So far, only three maternal effect genes (*Hsf1*, *Zar1*, and *Npm2*) have been shown to have an effect at the zygote–two-cell transition (28–30). The asynchronous fragmentation of *Gpr3*$^{-/-}$ zygotes is highly reminiscent of the *Zar1*$^{-/-}$ and *Npm2*$^{-/-}$ phenotypes (29, 30).

Aging *Gpr3*$^{-/-}$ Females Display Increased Follicle-Stimulating Hormone (FSH) Levels in Serum and Shorter Estrous Cycles. Reproductive aging in the woman is associated with increased FSH levels and shorter menstrual cycle (31). As an index of ovarian function, FSH levels were assayed in serum of 8.5-month-old *Gpr3*$^{-/-}$ and *Gpr3*$^{+/+}$ females during diestrus. Distribution of values was significantly different between *Gpr3*$^{-/-}$ and *Gpr3*$^{+/+}$ animals, with the former displaying a shift toward higher values ($P <$ 0.001 by Mann–Whitney test; see Fig. 5, which is published as supporting information on the PNAS web site). In the same way, we observed that *Gpr3*$^{-/-}$ females experienced shorter estrous cycles (+/+, 5.3 days ± 0.3; −/−, 4.3 days ± 0.1, $P < 0.001$ by Mann–Whitney test). These data qualify *Gpr3*$^{-/-}$ mice as a model of premature ovarian aging in women.

Conclusion

Together, our results indicate that the age-related reproductive failure of *Gpr3*$^{-/-}$ females can be fully explained by ovulation of a progressively increasing proportion of developmentally incompetent oocytes. They confirm that GPR3, probably via its ability to constitutively activate the cAMP regulatory cascade, plays an important synchronizing role during follicle development by contributing to the maintenance of meiotic arrest until the luteinizing hormone surge. However, the premature progression of *Gpr3*$^{-/-}$ oocytes through meiosis does not account for the age-dependent decrease in fertility, because it affects only a proportion of

eggs, which remains constant throughout the life of the animals. These observations are compatible with GPR3 playing an additional role in protecting or rescuing oocytes of older females from what we propose to call ''biochemical aging.'' Considering the Gs signaling activity of GPR3, it is tempting to hypothesize that this effect would be mediated by PKA-dependent phosphorylation of still unknown proteins (7). Interestingly, sphingosine 1-phosphate, which has been proposed as a putative GPR3 agonist, was shown to prevent developmental death of oocytes and preserve ovarian function *in vivo* (17, 32).

Gpr3$^{-/-}$ mice mimic, at an accelerated pace, the age-related decline of fertility in women, which manifests as a decreased monthly probability of conception, associated with increasing probability of pregnancy loss (33). In times when women are more and more delaying childbearing, the *Gpr3*$^{-/-}$ mouse model may become an invaluable tool for understanding the (patho)-physiology of ovarian aging in humans.

We thank L. Cuvelier, V. De Maertelaer, A. Delbaere, I. Huhtaniemi, F. Libert, P. Vanderhaeghen, and K. Van Wemmel for helpful discussions and significant input and L. Nebreda for technical assistance. This study was supported by the Belgian Program of Interuniversity Poles of Attraction (IUAP/PAI P5/30), initiated by the Belgian State Prime Minister's Office, Science Policy Programming. This work was also supported by grants from the Fonds de la Recherche Scientifique Médicale and Fonds National de la Recherche Scientifique. C.L., I.D., and D.B. are ''Chercheur Qualifié,'' ''Collaborateur Scientifique,'' and ''Chargé de Recherches'' of the Fonds National de la Recherche Scientifique, respectively.

1. Eppig, J. J., M. M. Viveiros, M. M., Marin Bivens, C. & De La Fuente, R. (2004) in *The Ovary*, eds. Leung, P. C. K. & Adashi, E. Y. (Elsevier, San Diego), pp. 113–129.
2. Sorensen, R. A. & Wassarman, P. M. (1976) *Dev. Biol.* **50,** 531–536.
3. Park, J. Y., Su, Y. Q., Ariga, M., Law, E., Jin, S. L. & Conti, M. (2004) *Science* **303,** 682–684.
4. Conti, M., Andersen, C. B., Richard, F., Mehats, C., Chun, S. Y., Horner, K., Jin, C. & Tsafriri, A. (2002) *Mol. Cell Endocrinol.* **187,** 153–159.
5. Bornslaeger, E. A., Mattei, P. & Schultz, R. M. (1986) *Dev. Biol.* **114,** 453–462.
6. Bornslaeger, E. A., Mattei, P. M. & Schultz, R. M. (1988) *Mol. Reprod. Dev.* **1,** 19–25.
7. Dekel, N. (1996) *Rev. Reprod.* **1,** 82–88.
8. Horner, K., Livera, G., Hinckley, M., Trinh, K., Storm, D. & Conti, M. (2003) *Dev. Biol.* **258,** 385–396.
9. Masciarelli, S., Horner, K., Liu, C., Park, S. H., Hinckley, M., Hockman, S., Nedachi, T., Jin, C., Conti, M. & Manganiello, V. (2004) *J. Clin. Invest.* **114,** 196–205.
10. Wiersma, A., Hirsch, B., Tsafriri, A., Hanssen, R. G., Van de, K. M., Kloosterboer, H. J., Conti, M. & Hsueh, A. J. (1998) *J. Clin. Invest.* **102,** 532–537.
11. Sallustri, A., Fulop, C., Camaioni, A. & Hascall, V. (2004) in *The Ovary*, eds. Leung, P. C. K. & Adashi, E. Y. (Elsevier, San Diego), pp. 113–130.
12. Dekel, N. (1988) in *Progress in Clinical and Biological Research*, eds. Haseltine, F. P. & First, N. L. (Liss, New York), pp. 87–101.
13. Mehlmann, L. M., Jones, T. L. & Jaffe, L. A. (2002) *Science* **297,** 1343–1345.
14. Kawamura, K., Kumagai, J., Sudo, S., Chun, S. Y., Pisarska, M., Morita, H., Toppari, J., Fu, P., Wade, J. D., Bathgate, R. A., *et al*. (2004) *Proc. Natl. Acad. Sci. USA* **101,** 7323–7328.
15. Saeki, Y., Ueno, S., Mizuno, R., Nishimura, T., Fujimura, H., Nagai, Y. & Yanagihara, T. (1993) *FEBS Lett.* **336,** 317–322.
16. Eggerickx, D., Denef, J. F., Labbe, O., Hayashi, Y., Refetoff, S., Vassart, G., Parmentier, M. & Libert, F. (1995) *Biochem. J.* **309,** 837–843.
17. Uhlenbrock, K., Gassenhuber, H. & Kostenis, E. (2002) *Cell Signal.* **14,** 941–953.
18. Mehlmann, L. M., Saeki, Y., Tanaka, S., Brennan, T. J., Evsikov, A. V., Pendola, F. L., Knowles, B. B., Eppig, J. J. & Jaffe, L. A. (2004) *Science* **306,** 1947–1950.
19. Sanfins, A., Lee, G. Y., Plancha, C. E., Overstrom, E. W. & Albertini, D. F. (2003) *Biol. Reprod.* **69,** 2059–2067.
20. Paria, B. C., Huet-Hudson, Y. M. & Dey, S. K. (1993) *Proc. Natl. Acad. Sci. USA* **90,** 10159–10162.
21. van Casteren, J. I. J., Schoonen, W. G. E. J. & Kloosterboer, H. J. (2000) *Biol. Reprod.* **62,** 886–894.
22. Ertzeid, G. & Storeng, R. (1992) *J. Reprod. Fertil.* **96,** 649–655.
23. Vogel, R. & Spielmann, H. (1992) *Reprod. Toxicol.* **6,** 329–333.
24. Fujino, Y., Ozaki, K., Yamamasu, S., Ito, F., Matsuoka, I., Hayashi, E., Nakamura, H., Ogita, S., Sato, E. & Inoue, M. (1996) *Hum. Reprod.* **11,** 1480–1483.
25. Tarin, J. J., Perez-Albala, S. & Cano, A. (2001) *Biol. Reprod.* **65,** 141–150.
26. Vom Saal, F., Finch, C. & Nelson, J. (1994) in *The Physiology of Reproduction*, eds. Knobil, E. & Neill, J. (Raven, New York), pp. 1213–1314.
27. Navot, D., Bergh, P. A., Williams, M. A., Garrisi, G. J., Guzman, I., Sandler, B. & Grunfeld, L. (1991) *Lancet* **337,** 1375–1377.
28. Christians, E., Davis, A. A., Thomas, S. D. & Benjamin, I. J. (2000) *Nature* **407,** 693–694.
29. Wu, X., Viveiros, M. M., Eppig, J. J., Bai, Y., Fitzpatrick, S. L. & Matzuk, M. M. (2003) *Nat. Genet.* **33,** 187–191.
30. Burns, K. H., Viveiros, M. M., Ren, Y., Wang, P., DeMayo, F. J., Frail, D. E., Eppig, J. J. & Matzuk, M. M. (2003) *Science* **300,** 633–636.
31. Sherman, B. M. & Korenman, S. G. (1975) *J. Clin. Invest.* **55,** 699–706.
32. Paris, F., Perez, G. I., Fuks, Z., Haimovitz-Friedman, A., Nguyen, H., Bose, M., Ilagan, A., Hunt, P. A., Morgan, W. F., Tilly, J. L., *et al*. (2002) *Nat. Med.* **8,** 901–902.
33. te Velde, E. R. & Pearson, P. L. (2002) *Hum. Reprod. Update* **8,** 141–154.